POINT CLOUD ACQUISITION BASED ON GNSS/SLAM WITH AN AUTONOMOUS BOAT IN URBAN RIVER ENVIRONMENTS

Masafumi Nakagawa*[1] , Naoto Kimura[2], Takeshi Komori[3], Nobuaki Kubo[3], Etsuro Shimizu[3]
[1]Professor, Department of Civil Engineering, Shibaura Institute of Technology,
3-7-5, Toyosu, Koto-ku, Tokyo, 135-8548, Japan
Email: mnaka@shibaura-it.ac.jp

[2]Graduate Student, Department of Civil Engineering, Shibaura Institute of Technology,
3-7-5, Toyosu, Koto-ku, Tokyo, 135-8548, Japan
Email: mh22006@shibaura-it.ac.jp

[3]Tokyo University of Marine Science and Technology,
2-1-6, Echujima, Koto-ku, Tokyo 135-8533, Japan

KEY WORDS: Indoor-outdoor seamless positioning, simultaneous localization and mapping, LiDAR, PPP-RTK, water-borne mobile mapping

ABSTRACT: Conventional autonomous boat navigation and water-borne 3D measurement systems depend on precise GNSS positioning. Therefore, in rivers located in densely populated urban areas, technical issues exist such as positioning errors under bridges because of poor Global Navigation Satellite System（GNSS) positioning environments. Thus, the authors focused on an integration of simultaneous localization and mapping (SLAM) and GNSS positioning techniques to achieve more stable positioning for autonomous boat control and 3D mapping in both GNSS and non-GNSS positioning environments. The proposed methodology involves using laser scanning and GNSS positioning as GNSS/SLAM to enable indoor-outdoor seamless positioning for autonomous boats and water-borne 3D measurement systems in rivers. Particularly, the authors focused on multi-layer LiDAR and precise point positioning based on real-time kinematic (PPP-RTK) positioning with the centimeter-level augmentation service (CLAS) to improve the performance of indoor-outdoor seamless positioning. The authors experimented with water-borne laser scanning and positioning in rivers to verify the performance of indoor-outdoor seamless positioning with GNSS/SLAM. Through the experiment, the authors confirmed that PPP-RTK positioning can be used for mobile mapping at rivers in dense urban areas.

1. INTRODUCTION

In the center of Tokyo, many navigable rivers by boat exist. We expect that urban rivers will be used more for transportation, logistics, sightseeing, and disaster management. Mobility as a service, which is a service that seamlessly connects various transportation systems to improve the convenience of movement, mainly focuses on the use of autonomous boats in water space, as well as services using autonomous driving cars. The operation of autonomous boats requires 3D maps of river spaces. However, there are currently no detailed 3D maps of river spaces. Therefore, a measurement platform for map creation is first required. Many autonomous boats use position data obtained through RTK-GNSS positioning for automated berthing and clash avoidance with LiDAR. However, urban rivers have a poor GNSS positioning environment because of the dense surroundings of buildings and bridges. Thus, technical issues remain in autonomous navigation using GNSS positioning. Therefore, we focus on indoor and outdoor seamless positioning methodology with a combination of GNSS positioning and self-position estimation using simultaneous localization and mapping (SLAM) using LiDAR (GNSS/SLAM) in urban rivers. For GNSS positioning in this study, we apply real-time kinematic (RTK) positioning with precision point positioning (PPP) methodology using a centimeter-level augmentation service (CLAS). The PPP-RTK using a CLAS receives an L6 signal from the quasi-zenith satellite Michibiki to reduce the effects of positioning errors caused by the ionosphere above the mobile station with reinforcement information (e.g. satellite clock and orbit information) calculated from electronic reference point data to obtain cm-level positioning results (Miura et al., 2020). Although the PPP-RTK using CLAS is a positioning service in Japan and the positioning accuracy is slightly lower than RTK-GNSS positioning, highly convenient data acquisition can be achieved because the positioning can omit the installation of a reference station and constant communication with the reference station. Moreover, the short time for re-FIX enables simplifying positioning mode switching in indoor-outdoor seamless positioning.

SLAM is a simultaneous processing of self-position estimation and point cloud acquisition. SLAM can be categorized by a main sensor, such as LiDAR-SLAM using LiDAR, Visual-SLAM using a camera, and Depth-SLAM using a time-of-flight (TOF) and depth camera. In most river measurements, the distance from a boat to measured objects is 5 m or more. Thus, the TOF camera has a disadvantage, and some issues exceed the measurable range of TOF and depth cameras: thus, LiDAR and cameras have the advantages of SLAM in river measurements. Moreover, urban rivers have large

brightness changes between open sky environments and non-GNSS positioning environments. Therefore, LiDAR has higher advantages than a camera for a main sensor of SLAM.

Indoor-outdoor seamless positioning is a technology to improve the availability of positioning in urban areas among GNSS and non-GNSS environments (Nakagawa, 2013). Because the service area of GNSS positioning is limited to open outdoor spaces, and the service range of indoor positioning is limited to indoor spaces and their surrounding areas, GNSS positioning is applied in outdoor spaces, and indoor positioning is applied in indoor spaces as the positioning mode. With a rapid change of positioning modes between GNSS and indoor positioning, we can improve the convenience of using spatial information services for pedestrian navigation. Indoor-outdoor seamless positioning is also an essential positioning technology for UAV flight control and autonomous mobile robot navigation. Indoor positioning, which is part of seamless indoor-outdoor positioning, can be classified into radio navigation and inertial navigation. Radio navigation is a methodology of position estimation for a moving object by a combination of receivers on the moving object and transmitters installed over a service area. Inertial navigation is a methodology of relative position estimation from a starting point using one or more sensors, such as acceleration sensors, gyro sensors, electronic compasses, cameras, and laser scanners. Examples of inertial navigation include pedestrian dead reckoning (Ichikari et al., 2018) and SLAM. While radio navigation requires indoor positioning infrastructure such as transmitters, inertial navigation does not require indoor positioning infrastructure. Urban rivers include non-GNSS environments, such as a space under a bridge, railway, or highway. Thus, indoor positioning techniques are required. However, radio navigation is currently not practical in such spaces because of the lack of indoor positioning infrastructure. Therefore, inertial navigation is better than radio navigation in urban rivers.

In previous research on waterborne mobile laser measurement, we have found technical issues, such as missing GNSS positioning measurements and degeneration problems in SLAM. A degeneration problem is a factor of failures in SLAM processing because of few geometrical features in 3D measurement. In this paper, we propose a methodology to perform the SLAM processing with indoor-outdoor seamless positioning and map matching, even if degeneration problems occur. GNSS positioning data cannot be obtained in a non-GNSS positioning environment. Therefore, we focused on the possibility of self-position estimation using map-matching processing on point clouds integrated by SLAM. Moreover, we verify the proposed methodology in experiments using a boat in urban areas.

2. METHODOLOGY

The proposed methodology, GNSS/SLAM (Figure 1), consists of initial position and orientation estimation using LiDAR, precise position and orientation estimation using SLAM, and dense point cloud generation (Nakagawa et al., 2020). The GNSS/SLAM consists of offline processing for mapping purposes and online processing for boat navigation. Navigation processing mainly consists of sequential LiDAR-SLAM and relocalization processing performed at arbitrary frame intervals (Figure 2). Relocalization processing is a process using map matching with scanning data using existing point clouds as a base map. The proposed methodology is based on indoor-outdoor seamless positioning using a combination of GNSS positioning and self-position estimation using SLAM using LiDAR (GNSS/SLAM).

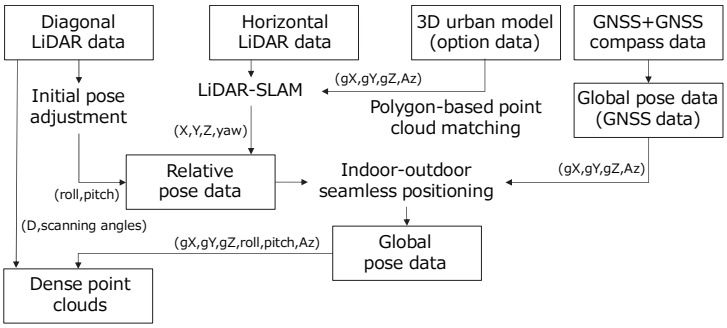

Figure 1. Proposed methodology

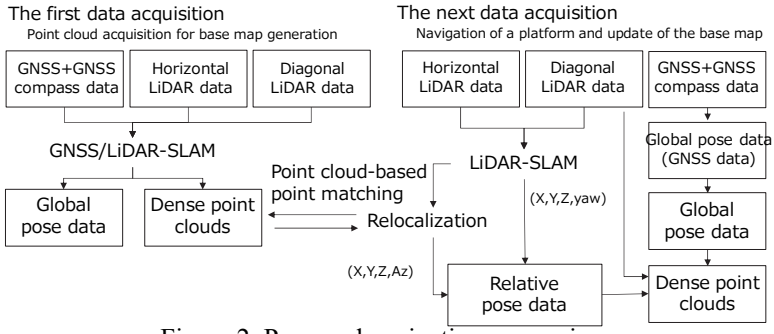

Figure 2. Proposed navigation processing

2.1 Initial pose estimation in GNSS/SLAM

GNSS/SLAM consists of processing for GNSS positioning environments (outdoor sections) and non-GNSS environments (indoor sections). In this study, the switching of positioning modes in seamless indoor-outdoor positioning is simplified with a GNSS positioning solution. Specifically, positions of RTK-FIX solutions are assumed as outdoor sections, and positions of RTK-Float solutions or worse are assumed as indoor sections. Furthermore, indoor sections are classified into short and long indoor sections. The navigation trajectory in a short indoor section is expected to be a straight line with a few meters to several tens of meters under a bridge. On the other hand, the navigation trajectory in a long indoor section is expected to be a free curved line with tens of meters to several kilometers under the expressway paralleled above the river. In the long indoor section, fine trajectory estimation is difficult. Therefore, first, a relative trajectory is estimated by SLAM. Next, GNSS positioning data are obtained at the endpoints of trajectory in GNSS environments. Then, georeference and error adjustment based on the open traverse is applied to the estimated relative trajectory using the endpoints of GNSS data to obtain the absolute trajectory.

In PPP-RTK and RTK-GNSS positioning, the positioning accuracy of the FIX solution is several centimeters. Based on this knowledge, in outdoor sections, the GNSS antenna position obtained through GNSS positioning is used for initial position estimation. In the short indoor section, the GNSS antenna position is estimated by linear interpolation processing from the GNSS positioning data acquired in the preceding and following outdoor sections, based on the fact that the navigation during the mobile measurement is constant speed navigation, as shown in Figure 3. The orientation (heading) of the GNSS antenna is also estimated using a baseline between any two local points on the trajectory estimated by GNSS positioning or interpolation. Although the heading cannot be estimated when the boat is stopped or rotating, mapping processing does not use data when the boat is stopped or rotating. Thus, if the moving speed can be estimated correctly, there are no problems with GNSS/SLAM. The initial position and orientation of LiDAR are estimated by rotation and translation of the offset value between the GNSS antenna and LiDAR with the initial position and orientation of the GNSS antenna estimated through indoor-outdoor seamless positioning.

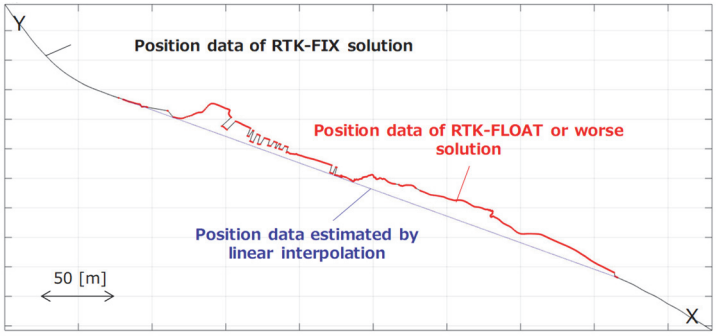

Figure 3. Initial pose estimation using GNSS positioning

GNSS/SLAM applies SLAM using the GNSS positioning results or the position estimated by interpolation processing as the initial position. With this approach, we aim to avoid the accumulated error problem in conventional SLAM processing. In conventional SLAM, accumulated errors are generally corrected by loop closure. However, in river measurements, loop closure cannot be applied because slightly turning a boat is difficult in urban rivers. Moreover, even if the circuit route can be designed for loop closure, the length of the loop is several kilometers to several tens of kilometers. Thus, the effect of accumulation error adjustment cannot be fully performed. Therefore, in our methodology, we use GNSS positioning results for initial position and orientation estimation in LiDAR-SLAM and indoor-outdoor seamless positioning.

2.2 Fine pose estimation in GNSS/SLAM

After the estimation of the initial sensor position, precise position and orientation are estimated with SLAM. In the GNSS positioning environments, the initial sensor position data are firstly determined by GNSS positioning. Next, the azimuth is rectified with SLAM. Then, the fine sensor position and orientation are estimated with SLAM. In non-GNSS positioning environments, although the initial position data given by indoor-outdoor seamless positioning are adjusted with the pose adjustment in SLAM, sensor position and orientation are also estimated in the SLAM.

SLAM is classified into the following three approaches. The first approach is SLAM with Bayesian filters, such as extended Kalman filter (EKF)-SLAM (Weingarten et al., 2005) and Rao-Blackwellized particle filter (RBPF)-SLAM (Murphy, 2000). The second approach is a graph-based SLAM with non-real-time optimization processing to optimize networks of sensor and feature positions. The third approach is a scan matching-based SLAM. EKF-SLAM has technical issues with scalability, and RBPF-SLAM is a 2D SLAM; thus, the first approach has poor scalability in point cloud processing. Moreover, graph-based SLAM is not suitable for river measurements because of the long edges in the pose graph. Therefore, in this study, we apply SLAM based on scan matching. SLAM based on scan matching is a real-time

processing SLAM that uses optimization calculations to align point clouds. Scan-matching-based SLAM can be classified into approaches with or without initial values. Represented approaches with initial values are the iterative closest point (ICP) algorithm (Chen et al., 1992) and the normal distributions transform (NDT) algorithm (Biber et al., 2003). An approach without initial values is the globally optimal ICP algorithm (Yang et al., 2016) that guarantees global optimization without providing an initial position. In this study, the ICP algorithm and NDT algorithm are strong candidates because the PPP-RTK results can be used as good initial values.

The ICP algorithm is a point cloud matching with iterative calculation of the relative position and orientation to minimize the distances of the base and corresponding point clouds. The ICP algorithm theoretically stays at a local optimal solution when the quality of the initial value is low. The NDT algorithm is a point cloud matching with a grid-based approach that approximates the set of points included in each grid using a normal distribution. The NDT algorithm has the advantage of low computational cost. In this study, we apply the ICP algorithm because we focus on the use of GNSS data as precise initial values preparation, omission of parameter settings such as grid size optimization, and higher accuracy in point cloud matching. However, conventional ICP algorithms have technical issues such as high computational costs depending on the amount of point clouds and weakness to spike noises in local optimization. Therefore, we improve calculation costs and redundancy against spike noise: that is, the ability to correctly match even point clouds containing noise, as shown in Figure 4.

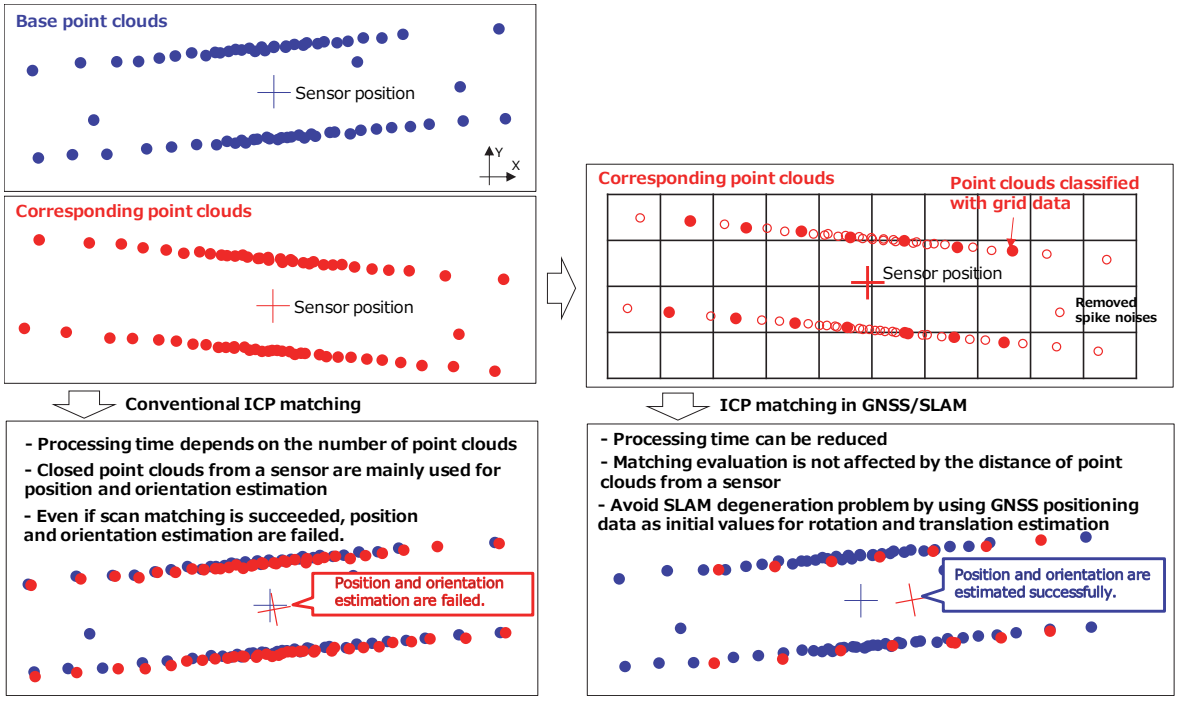

Figure 4. Improvement of the ICP algorithm in the proposed methodology

In the ICP algorithm, sampling either the reference data or the target data with geometrical feature point extraction is an effective idea to reduce computational costs without significantly reducing accuracy. However, when geometrical features are extracted from point clouds, including sparse and dense points depending on the distance from LiDAR, extraction results tend to be biased toward extraction from close-range point clouds where the geometry is represented. Therefore, in our feature extraction from point clouds for the ICP algorithm, we sampled point clouds to consist of near-far point clouds uniformly for stable scan matching. Specifically, first, a voxel space is prepared on point clouds. Next, representative points are selected from each voxel containing enough points. Then, the extracted point clouds are uniformly sampled. Based on these steps, calculation cost is improved with spike noise filtering in point cloud sampling for stable ICP processing.

Even if spike noise is removed through sampling processing, spike noises remain in either the reference data or the target data. Therefore, the redundancy against spike noises is improved by applying the least median of squares, which does not require pre-setting of thresholds for evaluation, to the evaluation function in point cloud matching.

In the highly accurate ICP algorithm, although the preprocessing normal estimation requires calculation time, a point-to-plane methodology is applied to find the rotation matrix and translation vector to minimize the sum of the squares of the distances between the point and the plane. Moreover, when using multilayer LiDAR, which can acquire point clouds containing information on multiple cross sections, a sufficient amount of point clouds can be acquired for SLAM, and highly accurate point cloud matching can be expected. Therefore, in this study, we apply point-to-point methodology, which calculates the rotation matrix and translation vector to minimize the sum of squares of the distances between corresponding points in the viewpoint of lower computational costs.

3. EXPERIMENT

We selected Sumida River (section A) as an open sky environment, Kanda River (section B) as a crowded sky environment by buildings, and Nihonbashigawa River (section C) as a non-GNSS environment blocked by buildings and urban expressways, as shown in Figure 5. Section B was selected for performance verification of indoor and outdoor seamless positioning. Section C was selected for performance verification of point cloud integration and navigation with GNSS/SLAM.

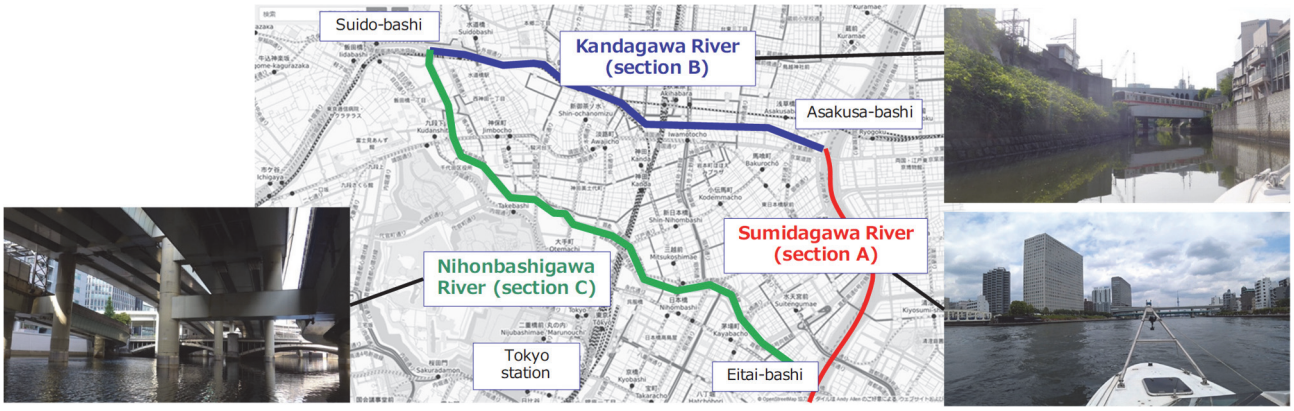

Figure 5. Measured sections

We selected several days and times when the tide level was low in Tokyo Bay to conduct experiments on rivers with almost no wind and calm wave conditions. We conducted on-water measurements from the battery-propelled vessel Raicho I, navigating at a speed of approximately 4.6 to 5.4 kn, and obtained GNSS positioning data by PPP-RTK positioning using CLAS and point clouds by laser scanning of horizontal and diagonal cross sections, as shown in Figure 6. For the PPP-RTK, we used a GNSS antenna (GPS-703-GGG-HV, NovAtel) and GNSS modules (AsteRx4 and mosaic-X5, Septentrio) with a 5 Hz sampling rate. We also acquired point clouds at 10 Hz with VLP-32C (Velodyne) for laser scanning of horizontal sections and VLP-16 (Velodyne) for laser scanning of diagonal sections. Moreover, positioning data (5 Hz) was obtained using RTK-GNSS positioning (ZED-F9P, u-blox) for accuracy verification. Additionally, although not covered in this paper, we also acquired video data from a front camera (HDR-AS300, Sony) and panorama images from an omnidirectional camera (Ladybug5, Teledyne FLIR) as reference data. We confirmed that the range of roll and pitch angles during the data acquisition was approximately ±3 degrees at maximum and 0.0 to 0.3 degrees at 0.2-second intervals from the laser scanning results.

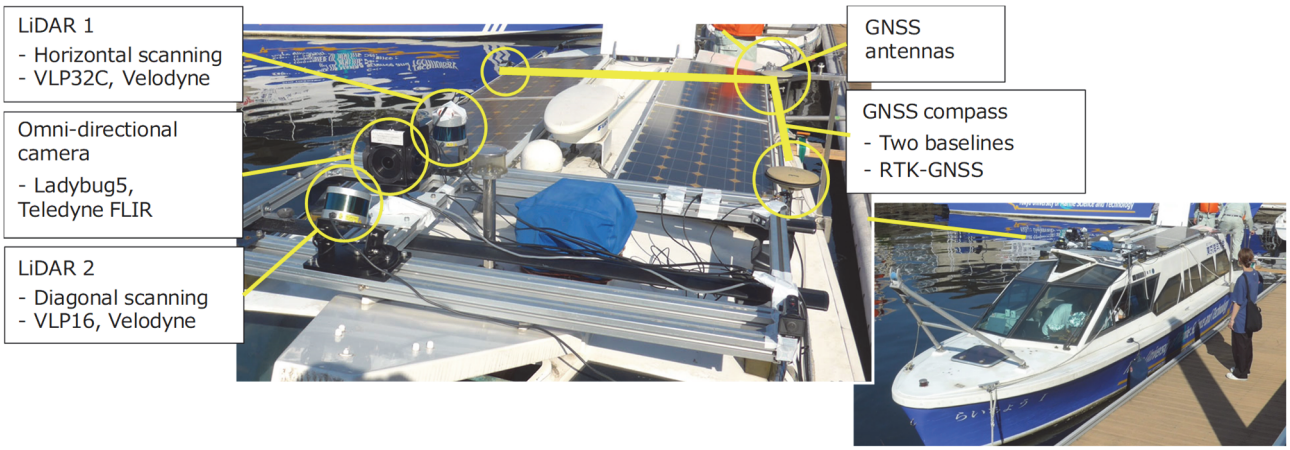

Figure 6. Measurement instruments for GNSS/SLAM

In the performance verification of point cloud integration and navigation with GNSS/SLAM, we used the first data (3000 frames, May 12, 2023, 12:00-14:00) for the base map and the second data (3000 frames, August 30, 2023, 9:00-11:00) for navigation verification. The point clouds for the base map were acquired in the upstream direction, and the poses were adjusted using the CLAS positioning data acquired at both the upstream and downstream ends. The point clouds for the navigation verification were acquired in the downstream direction, and the CLAS position data acquired at the start point in the GNSS positioning environment was used as the initial position for pose adjustment. In navigation verification, the scan-matching interval was set to 0.1 seconds (1 frame), and the map-matching processing interval was set to 10 to 40 seconds (100 to 400 frames).

4. RESULTS AND DISCUSSION

Acquired GNSS positioning results are shown in Figure 7. In section C (Nihonbashigawa River), RTK-FIX solutions for positioning were not obtained. In contrast, in sections A (Sumidagawa River) and B (Kanda River), RTK-FIX solutions were obtained except under bridges. Figure 8 shows the GNSS positioning results of AsteRx4 in section B (Kandagawa River) and the local sections for GNSS/SLAM inspection.

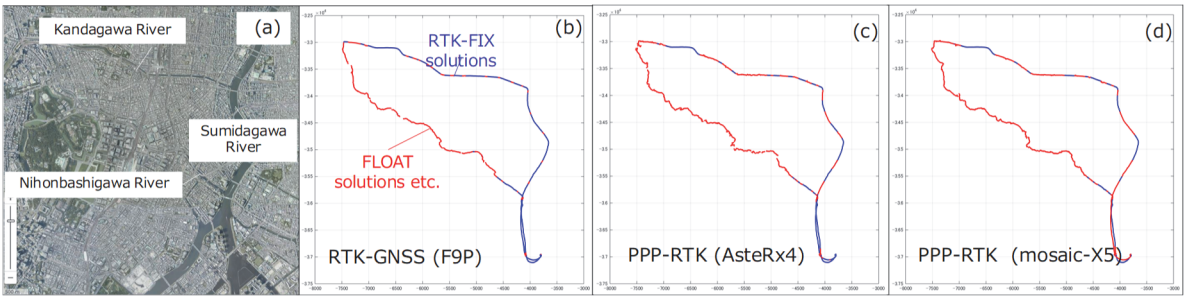

Figure 7. GNSS positioning results

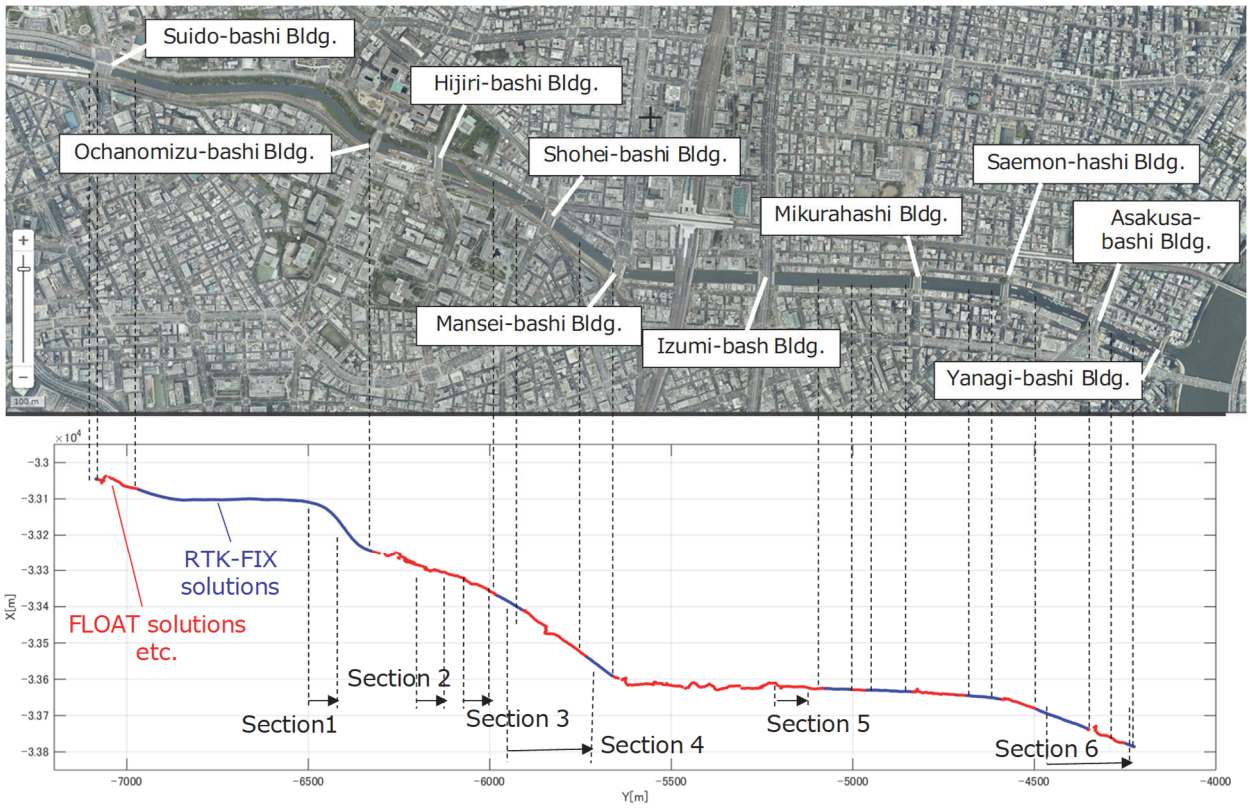

Figure 8. GNSS positioning results (AsteRx4) and local sections for GNSS/SLAM inspection in section B (Kandagawa River)

Table 1 shows the RTK-FIX rate of positioning results during laser scanning (31,500 epochs, 6,300 [s]: 9:37:30-11:22:30 (JST), December 3, 2021). Table 2 shows the accuracy verification results of the positioning results in GNSS positioning. Here, we used the RTK-GNSS positioning results as reference data and showed the root mean square error of the position obtained with the RTK-FIX solutions using both RTK-GNSS and PPP-RTK.

Table 1. RTK-FIX rate of PPP-RTK Accuracy verification results of PPP-RTK

		Positioning result : RTK-GNSS (F9P)		Comparison of PPP-RTK results	Total of PPP-RTK results
		The number of epochs (FIX solutions)	The number of epochs (FLOAT solution etc.)		
Positioning result: PPP-RTK(AsteRx4)	The number of epochs (FIX solutions)	15026 (47.7%)	13 (0.0%)	15039 (47.7%)	31500 (100.0%)
	The number of epochs (FLOAT solution etc.)	4608 (14.6%)	11854 (37.6%)	16462 (52.2%)	
Positioning result: PPP-RTK(mosaic-X5)	The number of epochs (FIX solutions)	11598 (36.8%)	33 (0.1%)	11631 (36.9%)	31500 (100.0%)
	The number of epochs (FLOAT solution etc.)	8036 (25.5%)	11834 (37.6%)	19870 (63.1%)	

Table 2. Accuracy evaluation results of PPP-RTK using RTK-GNSS positioning results as reference data

	PPP-RTK (AsteRx4)	PPP-RTK (mosaic-X5)
RMSE (XY)	0.035 [m]	0.025 [m]
RMSE (Z)	0.050 [m]	0.108 [m]

The quality of the results of self-position estimation in indoor-outdoor seamless positioning can be evaluated quantitatively using LiDAR position point sequence data obtained by an automatic tracking total station or point clouds obtained from ground measurements with a terrestrial laser scanner. However, the use of a total station or terrestrial laser scanner is inadequate because few places for the installation of instruments exist around rivers. Therefore, we conducted qualitative evaluation based on the accuracy of point cloud integration using ICP, and qualitative evaluation based on the continuity of estimated positioning positions and the deviation of the integrated point clouds. Based on the distance measurement accuracy of VLP-32C, we evaluated that the two types of PPP-RTK results have almost the same positioning accuracy. Thus, we used the positioning results of AsteRx4 as input data. We compared a conventional SLAM (without GNSS positioning) and the proposed methodology under the same conditions of the processing environment (MATLAB, CPU: Intel Core i7-10710U 1.10 GHz, RAM: 16 Gbytes) and the processing contents of scan matching. We selected the sections corresponding to the section numbers shown in Figure 8 from the point cloud obtained by horizontal scanning as input data. Then, we used the point clouds extracted within the height range of (-0.5 to 0.5) m from the horizontal LiDAR. The processing results for sections 1 to 4 are shown in Figure 9, and the processing results for sections 5 and 6 are shown in Figure 10.

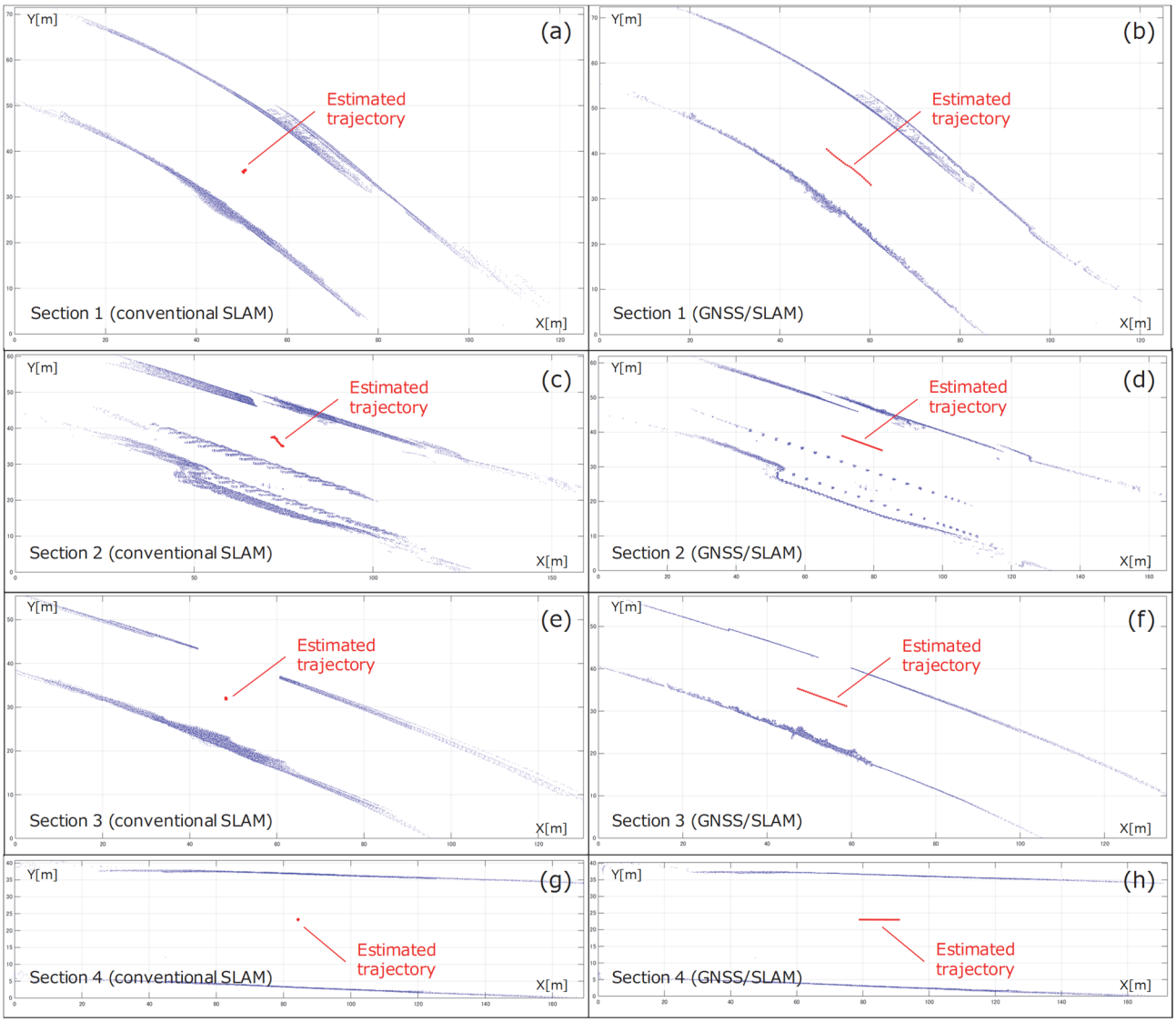

Figure 9. Point cloud processing results for local sections 1 to 4 (left column: conventional SLAM, right column: GNSS/SLAM)

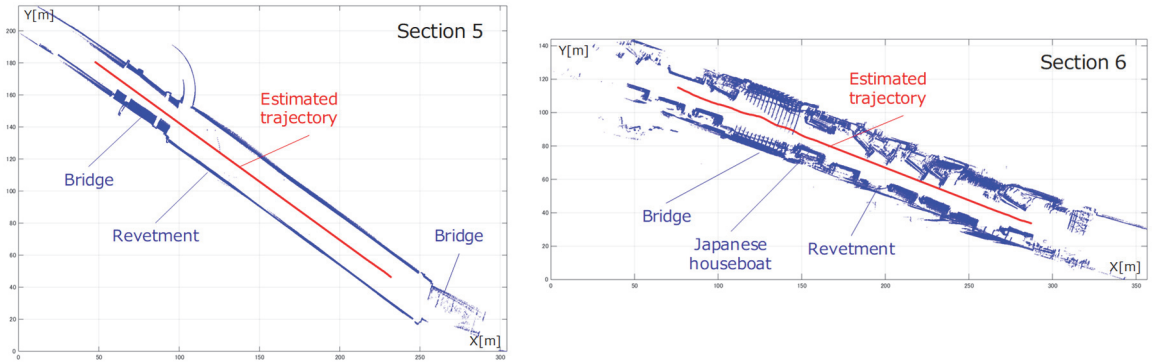

Figure 10. Point cloud processing results for local sections 5 and 6 (GNSS/SLAM)

As shown in Figure 9, the proposed methodology provided better results than the conventional SLAM. In conventional SLAM results, we confirmed that self-position estimation results were obtained; however, we also confirmed that self-position estimation tends to fail in areas around monotonous revetments or places under wide bridges, as shown in the left column of Figure 9. In contrast, the proposed methodology successfully estimated the self-position, even in areas where conventional SLAM failed, as shown in the right column of Figure 9. Moreover, Figure 10 shows that estimated position data were continuous in GNSS and non-GNSS environments, and features in point clouds were represented clearly. These results indicate that the failure of self-localization in the conventional SLAM was because of the degeneration problem in SLAM. Thus, we confirmed that the proposed methodology can avoid the degeneration problem in SLAM. Furthermore, we confirmed that PPP-RTK using CLAS can be used as an initial value for GNSS/SLAM, and can be used to acquire precise point clouds in urban rivers. We also confirmed that both conventional SLAM and the proposed methodology performed ICP processing for each scene as well as the distance measurement accuracy of LiDAR (Table 3).

Table 3. Point cloud integration accuracy in ICP processing

		Section 1	Section 2	Section 3	Section 4	Section 5	Section 6
Conventional SLAM	Average	0.036	0.044	0.024	0.028	0.034	0.051
	Median	0.037	0.041	0.024	0.029	0.031	0.048
GNSS/SLAM	Average	0.036	0.013	0.017	0.013	0.032	0.035
	Median	0.035	0.013	0.017	0.014	0.030	0.032

The integrated point clouds for the base map are shown in Figure 11. We extracted point clouds located at the height of 1.5 to 2.5 m above the water surface to use for the base map.

Figure 11. Integrated point clouds (Nihonbashigawa River)

The navigation verification results using the base map and point clouds obtained in the second data acquisition are shown in Figure 12 and Table 4. The input data are scanning data (temporal point clouds) at the same height as the base map after the height registration using the tide level change value (approximately 0.3 m) estimated by diagonal laser scanning. Figure 13 shows that sensor position rectification has been applied to the sequential LiDAR-SLAM through map-matching processing.

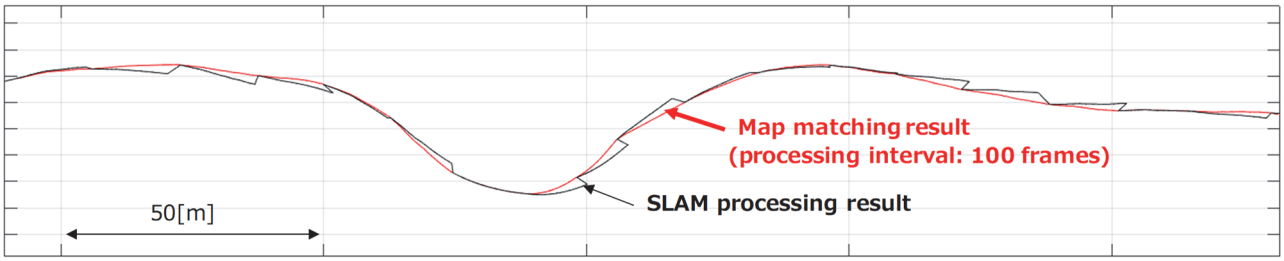

Figure 12. Verification result of navigation processing

Table 4. Processing time in navigation using point clouds

The number of scan positions	Relocalization intervals [scan position]	Relocalization intervals [sec]	Scan matching		Relocalization		Total [sec]
			Total [sec]	Average [sec]	Total [sec]	Average [sec]	
3000	100	10	223.94	0.07	58.78	1.90	282.72
3000	200	20	245.74	0.08	29.66	1.85	275.40
3000	300	30	226.23	0.08	19.40	1.76	245.63
3000	400	40	218.32	0.07	15.70	1.74	234.02

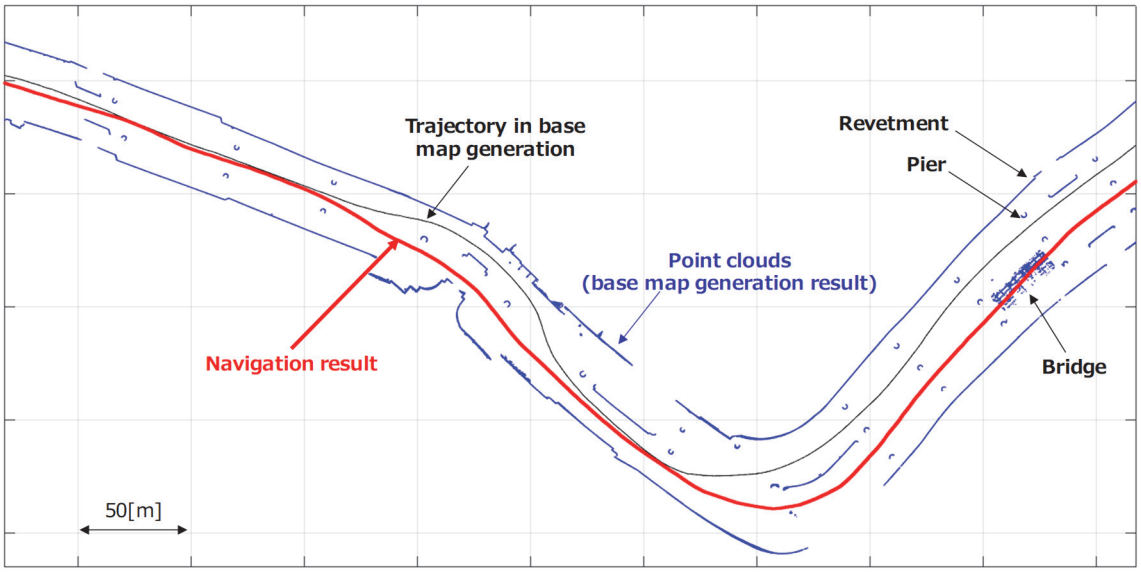

Figure 13. Sensor position rectification results in the navigation processing

5. SUMMARY

In this study, we proposed GNSS/SLAM to achieve indoor-outdoor seamless positioning and point cloud acquisition in urban rivers. We demonstrated that GNSS/SLAM can avoid the degeneration problem in SLAM, where conventional SLAM may fail in self-position estimation in rives, such as the space under bridges where positioning is missing, or near revetments with a monotonous shape. We also confirmed that PPP-RTK using CLAS can be used for mobile mapping in river space. We focused on the possibility of self-position estimation by map-matching processing on point clouds generated by NSS/SLAM, and we verified that the proposed methodology can achieve stable and rapid processing. The proposed methodology can also be used for UAVs for infrastructure inspections and autonomous mobile robots in indoor-outdoor environments.

ACKNOWLEDGMENTS

This research was supported by the MEXT Coordination Funds for Promoting AeroSpace Utilization; Grant Number JPJ21460038.

REFERENCES

Mimura, d., Miyatake, K., Kubo, Y., Sugimoto, S., 2020. Positioning Accuracy of Single Frequncy GNSS PPP by CLAS Comparing with MADOCA Products, Proceedings of the ISCIE International Symposium on Stochastic Systems Theory and its Applications, pp.43-48.

Nakagawa, M., 2013. Improvement in the Geofencing Service Interface Using Indoor Positioning Systems and Mobile Sensors, ISPRS Archives, Volume XL-4/W4, pp.27-30.

Ichikari, R., Shimomura, R., Kourogi, M., Okuma, T., Kurata, T., 2018. Review of PDR Challenge in Warehouse Picking and Advancing to xDR Challenge, 2018 International Conference on Indoor Positioning and Indoor Navigation (IPIN), pp. 1-8.

Nakagawa, M., Shinjiro Abe, S., Sanuka, S., Saito, K., Miyo, M., 2020. LiDAR Scan Matching with RTK-GNSS Positioning and Geometric Constraints, The 41st Asian Conference on Remote Sensing, 10 pages.

Weingarten, J., Siegwart, R., 2005. EKF-based 3D SLAM for Structured Environment Reconstruction, Proc. IEEE/RSJ International Conference on Intelligent Robots and System, pp.2089-2094.

P. Murphy, K., 2000. Bayesian Map Learning in Dynamic Environments, Advances in Neural Information, Processing Systems 12, pp.1015-1021.

Chen, Y., Medioni, G., 1992. Object Modelling by Registration of Multiple Range Images, Image Vision, Computing. Butterworth-Heinemann. Vol. 10, Issue 3, pp. 145-155.

Biber, P., Straßer, W., 2003. The Normal Distributions Transform: A New Approach to Laser Scan Matching, Proceedings of IEEE/RSJ International Conference on Intelligent Robots and Systems (IROS), Vol. 3, pp. 2743–2748.

Yang, J., Li, H., Campbell, D., Jia, Y., 2016. Go-ICP: A Globally Optimal Solution to 3D ICP Point-Set Registration, IEEE Transactions on Pattern Analysis and Machine Intelligence, 14 pages.